The evolution of magneto-transport and magneto-optical properties of thin $La_{0.8}Ag_{0.1}MnO_{3+\delta}$ films possessing the in-plane variant structure as a function of the film thickness

2006 J. Phys.: Condens. Matter 18 3753

(http://iopscience.iop.org/0953-8984/18/15/020)

INSTITUTE OF PHYSICS PUBLISHING JOURNAL OF PHYSICS: CONDENSED MATTER

J. Phys.: Condens. Matter **18** (2006) 3753–3765 doi:10.1088/0953-8984/18/15/020

The evolution of magneto-transport and magneto-optical properties of thin $La_{0.8}Ag_{0.1}MnO_{3+\delta}$ films possessing the in-plane variant structure as a function of the film thickness

O V Melnikov[1], Yu P Sukhorukov[2], A V Telegin[2], E A Gan'shina[1], N N Loshkareva[2], A R Kaul[1], O Yu Gorbenko[1], A N Vinogradov[1] and I B Smoljak[2]

[1] Lomonosov Moscow State University, 119992 Moscow, Russia
[2] Institute of Metal Physics, Ural Division of RAN, 620219 Ekaterinburg, Russia

E-mail: melnikov@inorg.chem.msu.ru

Received 24 November 2005
Published 30 March 2006
Online at stacks.iop.org/JPhysCM/18/3753

Abstract

Epitaxial $La_{0.8}Ag_{0.1}MnO_{3+\delta}$ films of different thicknesses (500–1000 nm) were grown on $ZrO_2(Y_2O_3)$ substrates. Their optical, magneto-optical and transport properties were studied in order to clarify the effect of the epitaxial variant structure and Ag ion distribution on the conductivity, magnetoresistance and infrared magnetotransmission in these films. An original method was developed for separating MR contributions related to the colossal magnetoresistance near T_C and the tunnelling magnetoresistance. It was established that in the $La_{0.8}Ag_{0.1}MnO_{3+\delta}$ films spin-polarization of electrons P reached ~0.5. The transverse Kerr effect revealed the irregular distribution of Ag ions through the film thickness. The comparison of optical and electrical data implies lower silver content near the film–substrate boundary in relation to that in the domain volume.

1. Introduction

The discovery of colossal magnetoresistance (CMR) and giant infrared (IR) magnetotransmission (GMT) [1, 2] in thin films of perovskite manganites resulted in new functional materials wherein the electrical and optical properties are controlled by the external magnetic field. Variation of the doping elements allowed for improving the CMR value and Curie temperature of the manganites. For example, doping $LaMnO_3$ by univalent cations Na^+ and Ag^+ led to the increase of T_C above room temperature [3–8] and CMR ~ 25% at 12 kOe near the Curie temperature [4]. Recently it has become clear that there is an additional contribution to magnetoresistance (MR) stemming from tunnelling of spin-polarized charge carriers in $La_{1-x}Ag_xMnO_3$

polycrystalline samples and $La_{0.8}Ag_{0.1}MnO_{3+\delta}$ (LAMO) epitaxial thin film possessing the in-plane variant structure [3–7, 9]. The tunnel magnetoresistance (TMR) was directly concerned with the transport through the random grain boundaries in polycrystalline materials or special high-angle boundaries in the films involving in-plane epitaxial variants. The contribution increased gradually under cooling below the magnetic phase transition. At 80 K in the polycrystalline material [4] tunnel magnetoresistance was ∼20% ($H = 10$ kOe) with $x = 0.165$ and ∼6% ($H = 4$ kOe) with $x = 0.1$ [9].

As shown by the present authors [9] the TMR was described by the function $f \sim 1/\sqrt{T}$ in the thin LAMO film possessing the in-plane variant structure, in contrast to $f \sim 1/T$ in granular and polycrystalline materials [10]. To optimize the high value of CMR and TMR in the films involving the in-plane variants it is necessary to study the thickness dependence of these parameters in the films and to estimate the distribution of Ag ions through the film thickness.

In the present work the comparative analysis of optical, magnetic, magneto-optical and transport properties of the $La_{0.8}Ag_{0.1}MnO_{3+\delta}$ films possessing the in-plane variant structure was accomplished to gain insight into the magneto-transport and magneto-optic response evolution as a function of the films thickness.

2. Samples and experimental conditions

Films different in the thickness d ($d = 500$, 800 and 1000 nm) were obtained under the same conditions with the original two-step procedure as described in [3]. At the first step $La_{0.8}MnO_{3+\delta}$ epitaxial films were grown by metallorganic chemical vapour deposition (MOCVD) on double-side polished single-crystal substrates of (001) $ZrO_2(Y_2O_3)$ (lattice parameter $a = 0.514$ nm). The deposition temperature for the $La_{0.8}MnO_{3+\delta}$ films was 800 °C, the precursor evaporation temperature 250 °C, the oxygen partial pressure 4 mbar and the total gas pressure 10 mbar (the deposition rate was about 10 nm min^{-1}). The second step consisted of the saturation of $La_{0.8}MnO_{3+\delta}$ films with silver by silver vapour treatment in an oxygen containing atmosphere. The treatment was done in the flow-through quartz reactor under 1 bar of oxygen pressure at a temperature of 800 °C. The samples were located on top of the ceramic boat filled with silver/porcelain mixture. During the process La vacancies in the perovskite lattice were filled by silver ions up to the mean composition $La_{0.8}Ag_{0.1}MnO_{3+\delta}$ as was concluded from the energy dispersion x-ray analysis (EDX). Note that the technique gives only the mean Ag content in the layer of the penetration depth thickness (∼1 μm). XPS (x-ray photoelectron spectroscopy) did not reveal any contribution of the metal silver in the film. According to the x-ray diffraction (XRD) measurements all films possessed the rhombohedral perovskite structure and the perovskite lattice spacing fluctuating in the range of about 3.889 ± 0.005 Å.

Using φ-scans for the asymmetric reflections of the film and the substrate we have found that the films grown on $ZrO_2(Y_2O_3)$ had pseudocubic (110) orientation but the fourfold variant structure appeared in the plane of the film. Each variant was characterized by the alignment of the volume diagonal of the perovskite cube along the face diagonal of the fluorite cube. As a result, thin films possessing such structure contained the high-angle boundaries (19.5°, 70.5° and 90°) between variant domains. But XRD reveals only the orientation and not the lateral size of the domains. By earlier HREM (high-resolution electron microscopy) study of the similar perovskite manganites we have shown that the lateral size of domains is typically 20–40 nm and only weakly dependent on the particular composition of the film [11]. The orientation relations of the variants as well as their ratio are fixed and do not vary through the film

Table 1. Film thickness (d), Curie temperature (T_C) measured at the film surface (SI)/at the film–substrate interface (BI), temperature of the resistivity maximum (T_ρ), temperature of IR radiation transmission (T_I) at the wavelength $\lambda = 6.7$ μm, temperature of the MR maximum (T_{MR}^{max}), temperature of the MT maximum (T_{MT}^{max}) and maximal values of CMR, MT and $TMR_{80\ K}$, measured in the field of 8 kOe, spin-polarization of charge carriers (P) and fitting parameter b for the epitaxial $La_{0.8}Ag_{0.1}MnO_3$ films grown on (001) $ZrO_2(Y_2O_3)$ single-crystal substrates.

d (nm)	T_C (K) SI/BI	T_ρ (K)	T_I (K)	T_{CMR}^{max} (K)	T_{MT}^{max} (K)	CMR (%)	MT (%)	TMR at 80 K (%)	P	b ($K^{1/2}$)
500	313/305	242	321	317	310	1.9	4	8.5	0.46	137
800	313/305	242	314	292	304	2.2	8	6.1	0.41	100
1000	313/298	203	285	276	285	2.4	7	9.4		

thickness. Moreover, HREM shows that the domain boundaries are structurally coherent along the normal to the film plane. This is the main distinction of the in-plane variant structure from the polycrystalline granular materials. This is why no strong peak broadening is observed in θ–2θ XRD patterns which are sensitive to the crystallite size in the film in the normal direction, but not in the lateral direction. The structure domains produce highly conducting ferromagnetic (FM) metallic nanodomains, separated by high-angle boundaries similar to the boundaries in the bicrystals [12]. For the LAMO films only TEM (transmission electron microscopy) data were available but they were in agreement with the results for other manganite systems obtained with the higher microscope resolution (size and uniformity in the alignment of the domains). Note that in the LAMO material possessing the variant structure the grain boundaries are normal to the film plane.

The optical properties of the films were determined by the high-sensitivity IR spectrometer in the wavelength range $0.8\ \mu m \leqslant \lambda \leqslant 14\ \mu m$ for the temperature from 80 to 380 K and magnetic field up to $H = 10$ kOe. Resistivity (ρ) was measured in the temperature range from 80 to 380 K and magnetic field up to $H = 10$ kOe. The transverse Kerr effect (δ) was studied in the energy range $1.2 < E < 4.2$ eV in the regime of heating up to 350 K, with the magnetic field up to 3.5 kOe. In such an experiment we have measured the relative change of the p-polarized light intensity reflected from the sample: $\delta = [I(H) - I(0)]/I(0)$, where $I(H)$ and $I(0)$ are the intensity of the reflected light with and without the magnetic field, respectively. Magnetic field was applied along the film plane. The measuring technique was described in detail previously [13]. The Kerr effect was measured with the direction of the incident light onto the film surface (SI) and onto the substrate back side (BI). Magnetization of the films was measured with the vibration magnetometer. Magnetic field was applied along the film plane.

3. Experiment

3.1. Transverse Kerr effect and magnetization

Both the temperature dependence of the transverse Kerr effect $\delta(T)$ in the SI mode and the magnetization $M(T)$ dependences show that the Curie temperature of all LAMO films (T_C) is 313 K (figures 1(a)–(c)). Variation of $M(T)$ in the low magnetic field (∼80 Oe) correlates with the variation of $\delta(T)$ for the films with the different thicknesses. In the BI mode the values of T_C are smaller especially for the films with the larger thickness (figures 1(b) and (d), table 1). For the film with the thickness 500 nm an anomalous variation of $\delta(T)$ with the Kerr effect sign inversion was observed in the temperature range 305–313 K (figure 1(d)). Such an anomaly in the temperature dependences near T_C was also observed in the dependence $\delta(T)$

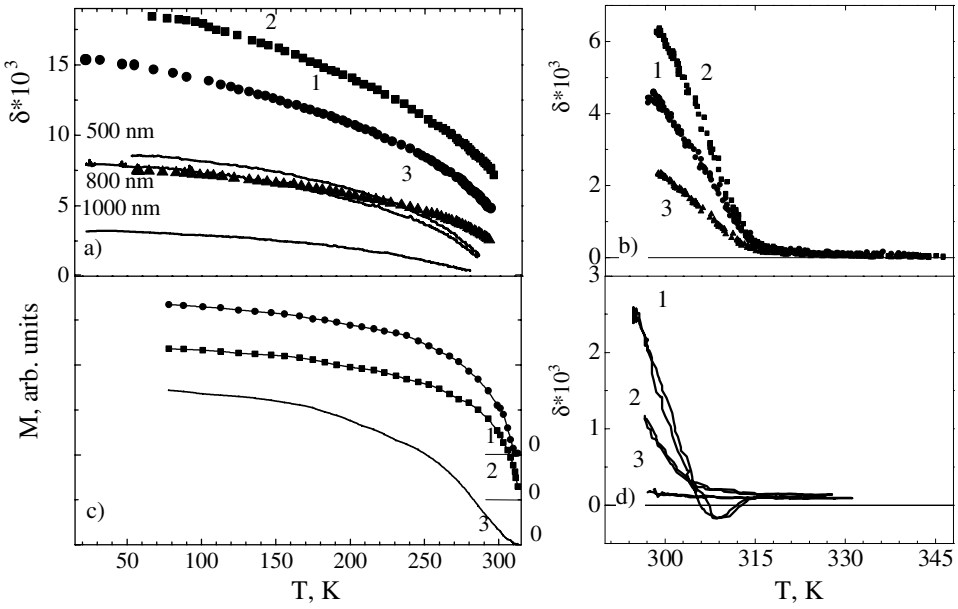

Figure 1. Temperature dependences: (a) transverse Kerr effect (δ) at 3.5 kOe, measured with SI on LAMO films with thicknesses 1—500 nm, 2—800 nm and 3—1000 nm, at the energy 2.95 eV (symbols) and with BI at 2.65 eV (lines); (b) δ for SI near T_C; (c) magnetizations (M) in the field 80 Oe (for easier viewing the plot zeros are shifted); (d) δ for BI near T_C.

for $(La_{0.5}Pr_{0.5})_{0.7}Ca_{0.3}MnO_3$ film on $SrTiO_3$ substrate [14] and for the single-crystal samples $La_{0.85}Sr_{0.15}MnO_3$ [16]. The difference in the temperature dependences of Kerr effect for SI and BI implies the magnetic non-uniformity of the films along the normal to the film surface.

Transverse Kerr effect (TKE) spectra measured for BI and SI were virtually the same for any thickness, but the effect magnitude depended on the film thickness (figure 2), although for the uniform films the effect magnitude should be independent of the thickness. Increasing the film thickness up to 800 nm was attended by the growth of TKE value for the basic negative maximum from $\delta \sim -15 \times 10^{-3}$ to $\sim -20 \times 10^{-3}$ (at 80 K). These values are typical of the TKE magnitude for the optimally doped manganites [14–19]. The further increase of the film thickness up to 1000 nm led to the decrease of δ by a factor of two. The appearance of TKE spectra was changed if measured at the substrate backside. The peaks of the spectra were shifted to the lower energy by approximately 0.3 eV. The TKE value was higher at the positive maximum and lower at the negative one for BI in comparison with SI.

Field dependences of the relative magnetization $m = M(T)/M_S$ of the LAMO films, calculated from the Kerr effect data at 80 K, were practically coincident for BI and SI (figure 3(a)) and demonstrated saturation at $H > 0.5$ kOe. However, the comparison of the magnetization curves, derived directly from the magnetic measurements of the films different in thickness, showed that magnetization of all films saturated in the lower field of ∼80 Oe at $T = 295$ K and ∼200 Oe at 80 K (see, for example, inset in figure 3(a) for the film of 800 nm thickness). The coercive force at 295 K was $H_c \approx 20$ Oe, but at 80 K it increased to 112 Oe. The Kerr effect value is proportional to the magnetization, and consequently proportional to the fraction of the FM phase in the near-surface layer. The increase of Kerr effect with the film thickness continues up to 800 nm and indicates the growth of the FM phase fraction (figure 3(b)). The further increase of the film thickness up to 1000 nm is attended by the

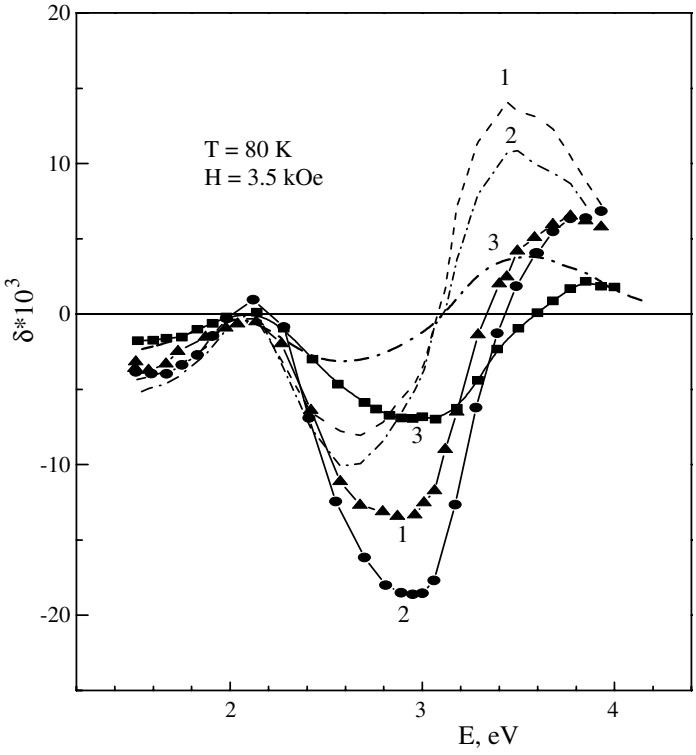

Figure 2. Spectra of the transverse Kerr effect (δ) in the LAMO films with different thicknesses: 1—500 nm, 2—800 nm, 3—1000 nm, measured in SI (symbols) and BI (lines) modes.

decrease of the transverse Kerr effect and, consequently, the decrease of the FM phase fraction in the near-surface layer.

3.2. Electrical properties and magnetoresistance

For LAMO films possessing the variant structure the temperature dependence of the resistance $\rho(T)$ revealed the broad apparent transition of the metal–insulator type (MI) (figure 4(a)). The temperature of the resistance maximum for the films 500 and 800 nm thick was the same ($T_\rho \approx 242$ K). In the film 1000 nm thick $T_\rho \approx 203$ K was found (table 1). The semiconductor-type curves of $\rho(T)$ have weak features at $T \approx 320$ K (for $d = 500$ nm), at 310 K ($d = 800$ nm) and at 285 K ($d = 1000$ nm). The smooth slope decline was observed in the $\rho(T)$ curve below T_ρ for all LAMO films. With the increase of the layer thickness up to 800 nm the resistivity decreased by a factor of two at T_ρ. The further increase of the film thickness up to 1000 nm resulted in 50 times higher resistivity.

The maximum of magnetoresistance $\mathrm{MR} = (\rho_H - \rho_0)/\rho_0 = \Delta\rho/\rho_0$ was related to the CMR effect observed near T_C (figure 5(a)). The CMR value slightly increased when the LAMO film thickness increased to 1000 nm but the temperature of the maximum ($T_\mathrm{CMR}^\mathrm{max}$) decreased. The increase of MR at the temperature well below T_C is related to the tunnel magnetoresistance, due to the high-angle boundaries of the structural domains in LAMO films involving the in-plane variants [9]. At 80 K the TMR value reached ∼9.4% at $d = 1000$ nm and ∼6.1% at $d = 800$ nm.

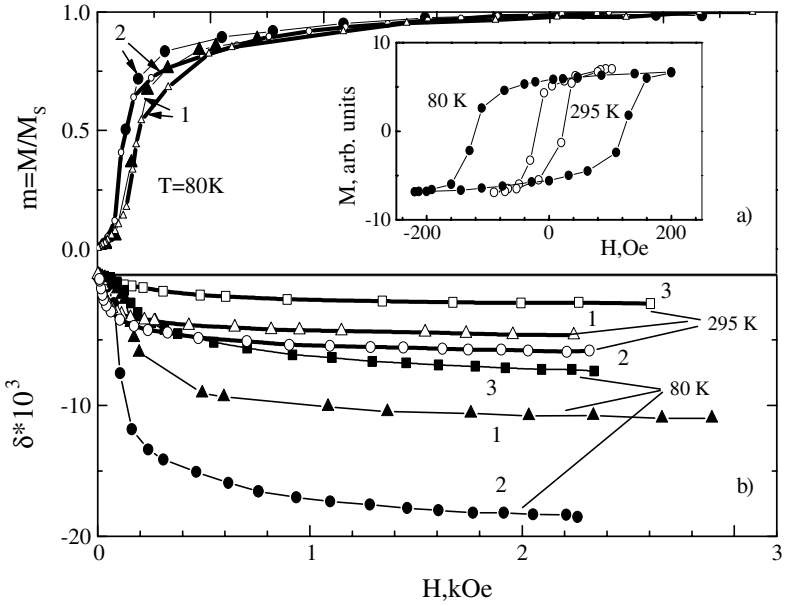

Figure 3. Field dependences: (a) relative magnetizations $m = M/M_S$, calculated from the Kerr effect for SI at the energy of 2.95 eV (solid symbols and thin line) and for BI at 2.65 eV (open symbols and thick line); (b) transverse Kerr effect of the LAMO films with thicknesses 1—500 nm, 2—800 nm and 3—1000 nm, measured at the different temperatures in the magnetic field parallel to the film plane. Inset—magnetization hysteresis loops of the film with $d = 800$ nm at the different temperatures.

The field dependences of CMR and TMR reveal different evolutions with the temperature variation. For example, the inset in figure 5(a) shows MR(H) dependences which were measured near $T_{\mathrm{CMR}}^{\mathrm{max}}$ and at 80 K in the film with $d = 800$ nm. In the field above 2 kOe the colossal magnetoresistance increased linearly with respect to H. It was only slightly dependent on the field orientation, along ($H_{\parallel}$) or normal ($H_{\perp}$) to the film surface, and had no hysteresis (which is typical for the CMR effect near T_{C}). In contrast, the TMR field dependence was substantially non-monotonic, had a hysteresis (butterfly-like loop) and depended on the magnetic field direction. The coercive force was $H_{\mathrm{c}} = 1.6$ kOe for $H_{\perp}$ in the films of 800 and 1000 nm thickness and $H_{\mathrm{c}} = 2.1$ kOe for $d = 500$ nm. For the parallel magnetization $H_{\mathrm{c}} \sim 250$ Oe was found, which was close to the H_{c} value deduced from the $M(H)$ dependence. The coercive force was determined as the half distance between the MR(H) maxima in a similar way to the H_{c} calculation for the heterostructure $La_{0.67}Sr_{0.33}MnO_3$/TB/$La_{0.67}Sr_{0.33}MnO_3$ with an $SrTiO_3$ tunnel barrier (TB) 4.4 nm thick [10]. The smaller H_{c} in the applied magnetic field in the plane of the film indicates predominantly in-plane anisotropy of the TMR.

3.3. Optical properties

The measurements of the transmission as a function of temperature $I(T)$ were performed at the fixed wavelength $\lambda = 6$ μm in the IR spectral range where the light interacts with free charge carriers. The relative optical transmission $I_{\mathrm{rel}}(T) = (I - I_{80\ \mathrm{K}})/I_{80\ \mathrm{K}}$ of $La_{0.8}Ag_{0.1}MnO_3$ films upon cooling down to ~200 K demonstrated a weak at first, but then more pronounced, metal-like behaviour (figure 4(b)) in spite of the semiconductor-like character of $\rho(T)$ in the same temperature range (figure 4(a)). The fractures appeared in $I_{\mathrm{rel}}(T)$ curves near ~320 K

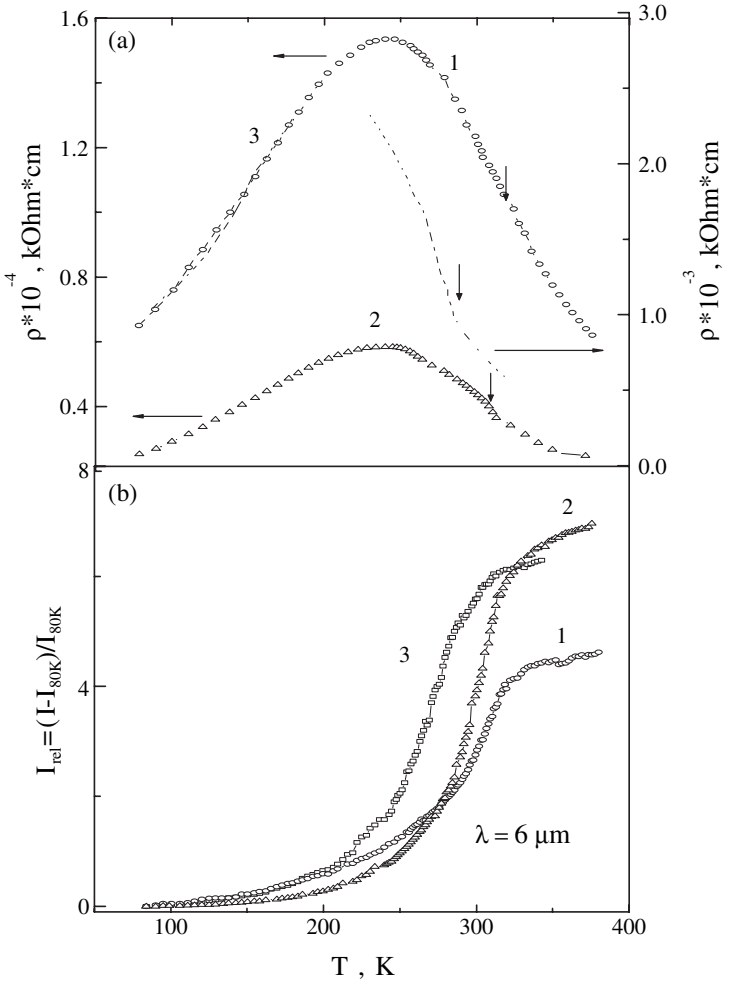

Figure 4. Temperature dependences: (a) resistivity (ρ); (b) the relative light transmission ($I_{\rm rel}$) at fixed wavelength for the LAMO films with the different thicknesses: 1—500 nm, 2—800 nm, 3—1000 nm. Vertical arrows denote the anomaly position on the $\rho(T)$ plots.

($d = 500$ nm), ∼310 K ($d = 800$ nm) and ∼285 K ($d = 1000$ nm), when the weak anomaly of $\rho(T)$ was observed too. In the film with $d = 800$ nm the characteristic temperature T_I of the curve fracture on the $I_{\rm rel}(T)$ curve is close to the Curie temperature measured for SI. In the thinner film ($d = 500$ nm) the relation $T_{\rm C} < T_I$ occurred, but in the thicker film ($d = 1000$ nm) $T_{\rm C} > T_I$ was found (see table 1).

Applied magnetic field decreased the transmission of IR radiation in the films near $T_{\rm C}$, i.e. negative magnetotransmission MT $= (I_H - I_0)/I_0$ took place, where I_H and I_0 are transmissions with and without the magnetic field, respectively. Figure 5(b) shows that MT(T) in the LAMO films measured at $\lambda = 6$ μm and $H = 8$ kOe possesses complicated behaviour: the presence of two maxima, a main one (its temperature and magnitude are listed in table 1) and a smaller additional one at lower temperature. With the increase of the film thickness up to 1000 nm the temperature of the main maximum of the magnetotransmission ($T_{\rm MT}^{\rm max}$) decreased in a similar way to $T_{\rm CMR}^{\rm max}$. The magnitude of the main MT maximum in the film

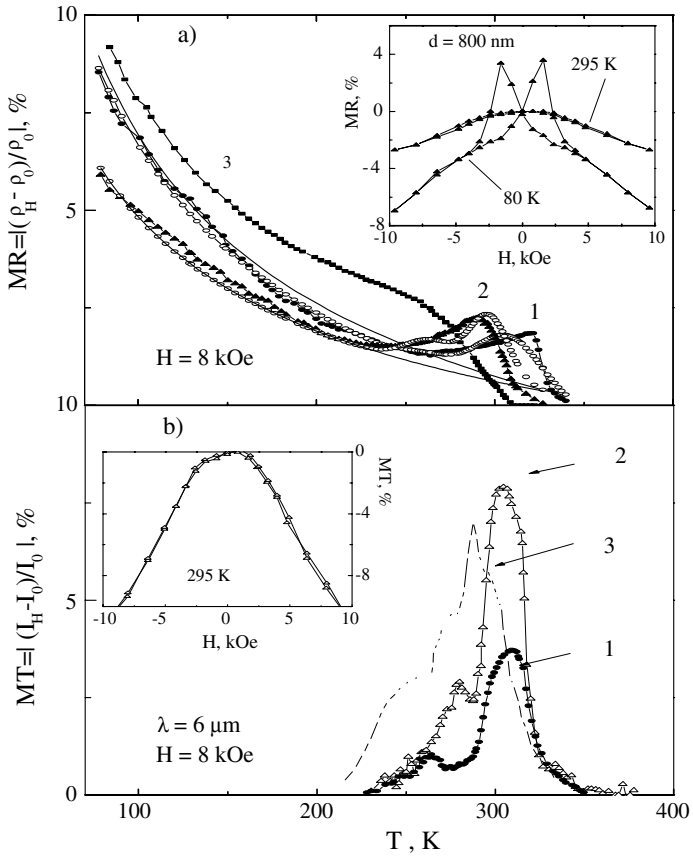

Figure 5. Temperature dependences: (a) the absolute value of the magnetoresistance (MR) and (b) the absolute value of magnetotransmission (MT) at fixed wavelength for the LAMO films with different thicknesses: 1—500 nm, 2—800 nm, 3—1000 nm. The functions $f = a + b/\sqrt{T}$ are denoted by the solid lines. Curves are obtained by fitting to the experiment MR data, using the $T_{\mathrm{MT}}^{\max}$ data, two analytical Gaussians and function $f = a + b/\sqrt{T}$—open circles (top panel). The insets show the MR field dependence (top panel) and MT field dependence (bottom one) for the film with $d = 800$ nm at different temperatures.

with $d = 800$ nm increased by a factor of two as compared to the film with $d = 500$ nm, and then decreased again for the film of 1000 nm thickness. The intensity of the additional peak only increased with the growth of the film thickness.

The magnetotransmission near T_{C} (inset in figure 5(b)) as well as CMR (inset in figure 5(a)) increased gradually for $H > 2$ kOe. MT depended only weakly on the magnetic field orientation along or normal to the plane of the film. Both MT and CMR had no hysteresis and no apparent saturation.

In the films with $d = 500$ nm and $d = 1000$ nm the remarkable increase of the absorption coefficient took place in the ferromagnetic state under cooling due to the growth of the light absorption by the free charge carrier (figure 6(b)). Magnetotransmission reached the high values in the broad IR spectral range from 1.5 to 9 μm at $T_{\mathrm{MT}}^{\max}$ and $H = 8$ kOe (figure 6(a)). The thickness variation did not result in the appearance of any new features in the MT spectra.

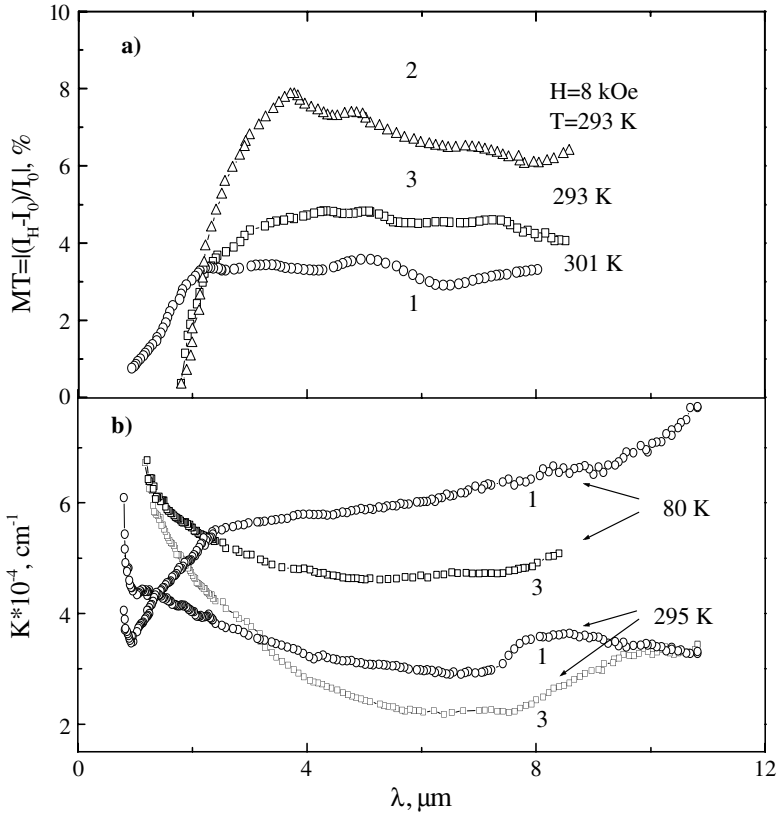

Figure 6. Spectra of (a) the magnetotransmission (MT) at T_{MT}^{max}; (b) the coefficient of light absorption (K) for the LAMO films with different thicknesses: 1—500 nm, 2—800 nm and 3—1000 nm.

4. Discussion of the results

The magneto-optic Kerr effect makes it possible to study the electronic and magnetic characteristics of the material in the thin skin layer ∼50 nm. The difference of Kerr effect for SI and BI modes, as well as non-monotonic variation of the effect magnitude with the thickness both for SI and BI, is evidence of the non-uniformity of the films in the transverse direction caused by the gradient distributions of Ag ions among the La vacancies through the film thickness. Kerr effect spectra for the LAMO films for BI at 80 K and the intensity correlation between the low-energy (∼2.7 eV) and the high-energy (∼3.1 eV) bands (figure 2) are retained. This is similar to material that is non-stoichiometric (La/Mn $<$ 1) or doped by the divalent ions Sr^{2+} and Ca^{2+} lanthanum manganite [14–19]. Bands in the TKE spectra are associated with competitive electro-dipole transitions in octahedral complexes MnO_6 with the different valence and spin-dependent d–d transitions in Mn^{4+} and Mn^{3+} ions [15, 16, 20]. The variable distributions of Ag ions among La vacancies through the film thickness leads to different ratios of Mn^{3+}/Mn^{4+} ions in the surface and substrate-film layers, i.e. to the presence of magnetic and structure non-uniformities. These peculiarities lead to the shift of the characteristic features in the Kerr effect spectra. The TKE spectra obtained for BI are similar to that of the epitaxial La_xMnO_3 film [19]. Noteworthily, the film surface with the higher silver content has higher T_C

compared to the film material near the film–substrate interface (silver penetrates from the gas phase and diffuses into the film in the direction from the surface to the film–substrate interface).

It was shown earlier [8, 9, 17–23] that the temperature variation of the IR radiation transmission near T_C for the optimally doped lanthanum manganites is the same as the temperature variation of the resistance at the MI transition. But in the case of the low doping the metallic phase volume is negligible and the sample stays insulating according to the $\rho(T)$ dependence. However, the $I(T)$ dependence demonstrates metallic-like behaviour below T_C associated with the volume fraction occupied by the FM metallic phase.

In the case of LAMO films structured by the epitaxial in-plane variants the crossover to the metallic-like transmission inside the structural domains starts at a higher temperature T_I than the apparent onset of metallic-like resistivity (T_ρ) (figure 4). Values of T_I are close to the temperature of weak features on the semiconductor-like branches of the $\rho(T)$ dependences for any film thickness (figure 4). This is evidence for the formation of FM metallic domains with high T_C, separated by the low T_C phase on the structure domains boundaries. This contribution was not detectable in the optical absorption because of the strong background of the metallic-like absorption. The flattened curve of $\rho(T)$ at $T < T_\rho$ can be attributed to the spin-dependent scattering of the charge carriers at the high-angle boundaries of structural domains starting at $T \approx T_I > T_\rho$.

With the increase of the film thickness up to 800 nm the LAMO film seems more uniform both electrically and magnetically. This is accompanied by the reduction of $\rho(T)$ (figure 4(a)), increase of T_ρ and weak change of T_I (see table 1). Obviously, at the further thickness increase up to 1000 nm, the film becomes less uniform again, which manifests itself in a significant decrease of both T_ρ and T_I and a strong increase of the electrical resistance, as well as a decrease of the Kerr effect (SI and BI) and a broader $M(T)$ dependence. The behaviour may be caused by the restricted silver penetration through the film thickness, which lead to a reduced silver concentration and even some remaining unreacted $La_{1-x}MnO_{3+\delta}$ material near the film–substrate interface. The latter is in agreement with TKE spectra of the $La_xMnO_{3+\delta}$ films [19]. The significant difference of the Kerr effect in SI and BI modes gives evidence for the gradient distribution of Ag ions through the film thickness.

Consequently, comparison of optical, magneto-optical and electrical data allows us to characterize the electronic and magnetic uniformity of the manganite films possessing the in-plane variant structure. An essential difference in the conduction mechanism becomes apparent from the comparison of the temperature dependences of the magnetoresistance and magnetotransmission.

Research on the large series of the lanthanum manganite films showed that magnetotransmission took place only near T_C [2, 17–23]. Magnetotransmission is the high-frequency analogue of the CMR. MT and CMR vary in parallel in the homogeneous materials. But in the magnetically heterogeneous sample MR is averaged over the whole material, while MT is related only to the metallic FM fraction. The presence of two maxima of MT in the films with $d = 500$ and 800 nm (figure 5(b)) means the co-existence of two FM phases with different T_C in these films. Note that the film of 1000 nm thickness reveals more complex $MT(T)$ behaviour, probably related to the larger number of the magnetic phases. It can be suggested that the existence of the phases with higher T_C is caused by doping $La_{0.8}MnO_3$ with silver ions, which can be absorbed up to $x \approx 20\%$ [3]. At the same time, the phase with the lower $T_C = 265$ K for $d = 500$ nm and $T_C = 275$ K for 800 nm is closer to La_xMnO_3 ($x = 0.83$) [19]. Since the lateral dimension of the structural domains is ~10 times less than the film thickness, it is unlikely that La_xMnO_3 remained inside domains near the film surface. But it is possible that the phase with lower T_C rests in the area near the film–substrate interface, where the silver penetration can be restricted by the slow diffusion kinetics or by the residual

epitaxial lattice strain near the film–substrate interface. Further exploration of this question demands chemical profile analysis of the film down to the film–substrate interface but it is ambiguous because of the possible silver loss under ion-beam etching [3].

In the LAMO films structured by the epitaxial variants MT disappears at $T < 220$ K, whereas MR(T) rises because of the tunnel magnetoresistance (figure 5). Respectively, the comparison of MR and MT data makes it possible to separate the contribution related to TMR.

The MT depends on the film thickness according to the equation $MT \approx \exp(-\Delta K d) - 1$, where ΔK is the difference of the absorption coefficients with and without the magnetic field (without taking reflection into consideration). In this case, the growth of the film thickness from 500 to 800 nm should increase the maximum MT value by a factor of two, which takes place in the wide IR spectral range (table 1, figures 5(b), 6(a)). In spite of the further growth of the film thickness up to 1000 nm, MT decreased, indicating the reduction of the high T_C phase fraction in agreement with the decrease of the Kerr effect magnitude (figure 1(a)) and broadening of the $M(T)$ dependence (figure 1(b)).

Keeping in mind that the magnetotransmission near T_C is an analogue of the magnetoresistance, and using parameters of two magnetic phases determined from the MT(T) dependence, we analysed the MR(T) curves for the LAMO films with $d = 500$ and 800 nm by the Gaussian fitting. In a wide temperature range the MR(T) dependence can be described as a sum of the contributions of the CMR peak near T_C and the tunnel MR; the latter increases with the temperature decrease (figure 5(a)). But we have not reached any satisfactory description of the MR(T) dependence of the 1000 nm film because of the larger number of oscillators needed.

For the TMR contribution the following function was used:

$$\Delta\rho/\rho_0 = a + b/\sqrt{T}, \tag{1}$$

where a is a temperature-independent member. Values of the fitting constant b are listed in table 1. Function (1) is different from the expression $f = a + b/(T + c)$ for the polycrystalline $La_{2/3}Sr_{1/3}MnO_3$ [24] and from the expression for the TMR in the ferromagnetic metallic granular films $\Delta\rho/\rho = -(JP/4k_BT)[m^2(H,T) - m^2(H,0)]$, where J is the exchange interaction constant, P the spin-polarization of electrons and m the magnetization, normalized to the saturation magnetization [10, 25, 26]. Function (1) determines the temperature dependence, which usually describes the magnetoresistance in a nanostructured material owing to the correlated tunnelling of spin-polarized electrons between the large grains by the nanograin chain with the appreciably smaller size [10, 27]. For the chains ordered in such material parallel to the current,

$$\Delta\rho/\rho_0 \approx -P^2m^2(1 + \sqrt{(C/T)}), \tag{2}$$

where C is a constant, depending on the excess Coulomb energy of a small grain in the chain loaded by an electron, and on the tunnel barrier parameters. Such a model accords better with the ordered character of the boundaries between the variant nanodomains in our LAMO films of different thicknesses, rather than with random boundaries in the bulk ceramic materials [24]. Earlier we have shown already that in the LAMO film possessing the variant structure with the thickness of 760 nm, the TMR is described by the function $f \sim 1/\sqrt{T}$ [9].

MR(T) curve extrapolation to the ordinate axis implies that TMR should reach ~55% (for $d = 500$ nm) and ~40% (for $d = 800$ nm) at $T = 2$ K. These values are close to the experimental TMR value of ~50% for the polycrystalline LAMO [5]. The TMR value at $T \sim 0$ K allows us to estimate the spin-polarization of electrons by the expression $\Delta\rho/\rho_0 = 2P^2/(1 - P^2)$ [10]: $P = 0.41$–0.46 in these LAMO films (table 1). The obtained spin-polarization of electrons is close to the value $P \sim 0.5$ of the film $La_{0.8}Ag_{0.1}MnO_{3+\delta}$ with the thickness of 760 nm, possessing the variant structure also [9]. Consequently, in the LAMO films structured by the in-plane epitaxial variants the spin-polarization P of electrons is ~0.5.

Since MT is the analogue of CMR, the CMR and MT field dependences are of the same type. The increase of the film thickness does not introduce any essential difference in the field dependences of these effects. The weak dependence of CMR and MT on the magnetic field orientation and monotonic dependence on the field magnitude correspond to the fluctuations of the magnetic moments near T_C. The appearance of the hysteresis of MR in the magnetic field dependence at low temperature (inset in figure 5(a)) can be attributed only to the tunnel MR in the presence of the variant structure in the LAMO films. The value of positive TMR $\sim 3\%$ ($d = 500$ and 800 nm) in the magnetic field of 250 Oe parallel to the film plane (inset in the figure 5) can be used in practice. The large value of the IR-radiation magnetotransmission, and the large Kerr effect in the visible range of spectra, giant negative tunnel magnetoresistance at low temperatures and CMR near the room temperature, can be used for the technical applications of this material.

5. Conclusions

The investigation of optical, magneto-optical and electrical properties of $La_{0.8}Ag_{0.1}MnO_{3+\delta}$ possessing variant structure and different thicknesses showed that with the increase of the film thickness up to $d = 800$ nm the LAMO film becomes more uniform both electrically and magnetically. At $d > 800$ nm the restricted silver penetration through the film thickness takes place. The gradient silver distribution among La vacancies through the film thickness leads to different magneto-optical responses for SI and BI because of the different Mn^{3+}/Mn^{4+} ion ratios in the skin layers. The film surface with the higher silver content produces higher T_C as compared to the film material near the film–substrate interface with the lower silver content. The crossover to the metallic-like transmission inside the structural domains starts at the higher temperature $T_I > T_\rho$, but the semiconductor-like behaviour of $\rho(T)$ dependence is determined by the high-angle boundaries. The comparison of optical and electrical data makes it possible to separate the MR contribution related to the colossal magnetoresistance near T_C and another one related to the tunnelling of spin-polarized carriers through the high-angle boundaries of the structure domains. The temperature dependence of the TMR can be described by the function $\Delta\rho/\rho_0 = a + b/\sqrt{T}$. The degree of spin polarization of charge carriers in the LAMO films is about 0.5. High values of the effects in $La_{0.8}Ag_{0.1}MnO_{3+\delta}$ films structured by the epitaxial in-plane variants, like positive TMR in low fields, negative TMR at low temperature in higher fields, and CMR near room temperature, as well as IR magnetotransmission and Kerr effect in the visible range of the spectra, can be used in various technical applications.

Acknowledgments

This work was supported by the RAS programme ‘New materials and structures’ and RFBR (grant Nos 04-02-16630 and 06-03-33070).

References

[1] von Helmolt R, Wecker J, Holzapfel B, Schultz L and Samwer K 1993 *Phys. Rev. Lett.* **71** 2331–3
[2] Sukhorukov Yu P, Loshkareva N N, Gan’shina E A, Kaul A R, Gorbenko O Yu and Fatieva K A 1999 *Tech. Phys. Lett.* **25** 551–4
[3] Gorbenko O Yu, Melnikov O V, Kaul A R, Babushkina N A and Barranco A 2005 *Electrochem. Soc. Proc.* **2005–09** 905–12
[4] Ye S L, Song W H, Dai J M, Wang K Y, Wang S G, Zhang C L, Du J J, Sun Y P and Fang J 2002 *J. Magn. Magn. Mater.* **248** 26–33

[5] Pi L, Hervieu M, Maignan A, Martin C and Raveau B 2003 *Solid State Commun.* **126** 229–34
[6] Gorbenko O Yu, Melnikov O V, Kaul A R, Balagurov A M, Bushmeleva S N, Koroleva L I and Demin R V 2005 *Mater. Sci. Eng.* B **116** 64–70
[7] Tao T, Cao Q Q, Gu K M, Xu H Y, Zhang S Y and Du Y W 2000 *Appl. Phys. Lett.* **77** 723–5
[8] Sukhorukov Yu P, Loshkareva N N, Telegin A V, Mostovshchikova E V, Kuznetsov V L, Kaul A R, Gorbenko O Yu, Gan'shina E A and Vinogradov A N 2003 *Tech. Phys. Lett.* **29** 904–6
[9] Sukhorukov Yu P, Telegin A V, Gan'shina E A, Loshkareva N N, Kaul A R, Gorbenko O Yu, Mostovshchikova E V, Melnikov O V and Vinogradov A N 2005 *Techn. Phys. Lett.* **31** 484–7
[10] Ziese M 2002 *Rep. Prog. Phys.* **65** 143–249
[11] Kaul A R, Gorbenko O Yu and Kamenev A A 2004 *Russ. Chem. Rev.* **73** 861–80
[12] Gorbenko O Yu, Demin R V, Kaul A R, Koroleva L I and Szymczak R 1998 *Phys. Solid State* **40** 263–7
[13] Balykina E A, Gan'shina E A and Krinchik G S 1987 *JETP* **93** 1879
[14] Gan'shina E A, Rodin I K, Loshkareva N N, Sukhorukov Yu P and Mostovshchikova E V 2002 *Bull. Russ. Acad. Sci.: Phys.* **66** 767–73
[15] Balykina E A, Gan'shina E A, Krinchik G S, Trifonov A Yu and Troiniachuk I O 1992 *J. Magn. Magn. Mater.* **117** 259–69
[16] Gan'shina E A, Vashuk H V, Vinogradov A N and Mukovskii Ya M 2004 *Symposium EASTMAG-2004 (Krasnoyarsk, Russia, 2004)* p 231 Book of abstracts
[17] Sukhorukov Yu P, Loshkareva N N, Gan'shina E A, Kaul A R, Gorbenko O Yu, Mostovshchikova E V, Telegin A V, Vinogradov A N and Rodin I K 2004 *Phys. Solid State* **46** 1241–51
[18] Sukhorukov Yu P, Gan'shina E A, Belevtsev B I, Loshkareva N N, Vinogradov A N, Rathnayaka K D D, Parasiris A and Naugle D G 2002 *J. Appl. Phys.* **91** 4403–8
[19] Sukhorukov Yu P, Loshkareva N N, Gan'shina E A, Mostovshchikova E V, Rodin I K, Kaul A R, Gorbenko O Yu, Bosak A S, Moskvin A S and Zenkov E V 2003 *JETP* **96** 257–67
[20] Loshkareva N N, Sukhorukov Yu P, Gan'shina E A, Mostovshchikova E V, Kumaritova R Yu, Moskvin A S, Panov Yu D, Gorbenko O Yu and Kaul A R 2001 *JETP* **92** 462–73
[21] Loshkareva N N, Solin N I, Sukhorukov Yu P, Lobachevskaya N I and Panfilova E V 2001 *Physica* B **293** 390–3
[22] Loshkareva N N, Sukhorukov Yu P, Naumov S V, Solin N I, Smoliak I B and Panfilova E V 1998 *JETP Lett.* **68** 97–100
[23] Sukhorukov Yu P, Nossov A P, Loshkareva N N, Mostovshchikova E V, Telegin A V, Favre-Nicolin E and Ranno L 2005 *J. Appl. Phys.* **97** 103710
[24] Hwang H Y, Cheong S-W, Ong N P and Batlogg B 1996 *Phys. Rev. Lett.* **77** 2041
[25] Helman J S and Abeles B 1976 *Phys. Rev. Lett.* **37** 1429–32
[26] Gittleman J I, Goldsrein Y and Bozowski S 1972 *Phys. Rev.* B **5** 3609–21
[27] Mitani S, Takahashi S, Takanashi K, Yakushiji K, Maekawa S and Fujimori H 1998 *Phys. Rev. Lett.* **81** 2799–802